Nucleic Acids Research, 2006, Vol. 34, No. 6 ***e50***
doi:10.1093/nar/gkl134

Molecular beacons with intrinsically fluorescent nucleotides

Angel A. Martí[1], Steffen Jockusch[1], Zengmin Li[2,3], Jingyue Ju[2,3] and Nicholas J. Turro[1,2,*]

[1]Department of Chemistry and [2]Department of Chemical Engineering, Columbia University, New York, NY 10027, USA and [3]Columbia Genome Center, Columbia University College of Physicians and Surgeons, New York, NY, 10032, USA

Received September 1, 2005; Revised November 23, 2005; Accepted March 14, 2006

ABSTRACT

We report the design, synthesis and characterization of a novel molecular beacon (MB-FB) which uses the fluorescent bases (FB) 2-aminopurine (AP) and pyrrolo-dC (P-dC) as fluorophores. Because the quantum yield of these FB depend on hybridization with complementary target, the fluorescent properties of MB-FB were tuned by placing the FB site specifically within the MB such that hybridization with complementary sequence switches from single strand to double strand for AP and vice versa for P-dC. The MB-FB produces a ratiometric fluorescence increase (the fluorescence emission of P-dC over that of AP in the presence and absence of complementary sequence) of 8.5 when excited at 310 nm, the maximum absorption of AP. This ratiometric fluorescence is increased to 14 by further optimizing excitation (325 nm). The fluorescence lifetime is also affected by the addition of target, producing a change in the long-lived component from 6.5 to 8.7 ns (Exc. 310 nm, Em. 450 nm). Thermal denaturation profiles monitored at 450 nm (P-dC emission) show a cooperative denaturation of the MB-FB with a melting temperature of 53°C. The thermal denaturation profile of MB-FB hybridized with its target shows a marked fluorescence reduction at 53°C, consistent with a transition from double stranded helix to random coil DNA.

INTRODUCTION

The development of efficient DNA and RNA fluorescence probes is an active area of research due to their application in genetic analysis (1), cellular imaging (2,3) and biomedical research (4,5). One of the most versatile probes for DNA and RNA detection are the fluorescent molecular beacons (MBs) (6,7). In general, a MB is a single stranded nucleic acid chain that forms a stem–loop structure. The loop is complementary to a target sequence, while the stem is labeled with a fluorophore and a quencher at the different ends of the strand (Scheme 1a). This MB sequence is designed, such that the last five or six bases at both ends of the oligonucleotide chain are complementary to each other bringing the fluorophore and the quencher close together when the double stranded (ds) structure (stem) is formed (8). In this configuration, the fluorescence is inhibited by the proximity of the fluorophore to the quencher, which provides non-radiative pathways for the deactivation of its excited state (9). In the presence of the target sequence, the MB undergoes a structural reorganization by hybridization of the loop with the target sequence leading to the formation of a ds helix and consequently in the spatial separation of the fluorophore and the quencher (Scheme 1a). In this new configuration, because of the large distance separation between the fluorophore and the quencher, the excited state of the fluorophore is not deactivated and a fluorescence signal can be detected (9). Under the same loop–stem principle, MBs with two fluorophores have been synthesized in which fluorescence resonance energy transfer (FRET) can be harvested to produce a distinctive fluorescence signal for the open and close states of the MB (10). Many other variations of MBs have also been explored (2,11–13), all sharing several features such as a loop–stem architecture, a distinctive fluorescence signal upon hybridization with the target and high sequence specificity (1–13).

Other molecular probes based on the MB concept have also been used to study DNA and RNA dynamics and interactions (14–16). One approach involves the use of single stranded (ss) oligonucleotides (complementary to a target sequence) possessing intrinsically fluorescent bases (FB) (17). A common fluorescent base is 2-aminopurine (AP) which, contrary to

*To whom correspondence should be addressed. Tel: +1 212 854 2175; Fax: +1 212 932 1289; Email: njt3@columbia.edu

© The Author 2006. Published by Oxford University Press. All rights reserved.

The online version of this article has been published under an open access model. Users are entitled to use, reproduce, disseminate, or display the open access version of this article for non-commercial purposes provided that: the original authorship is properly and fully attributed; the Journal and Oxford University Press are attributed as the original place of publication with the correct citation details given; if an article is subsequently reproduced or disseminated not in its entirety but only in part or as a derivative work this must be clearly indicated. For commercial re-use, please contact journals.permissions@oxfordjournals.org

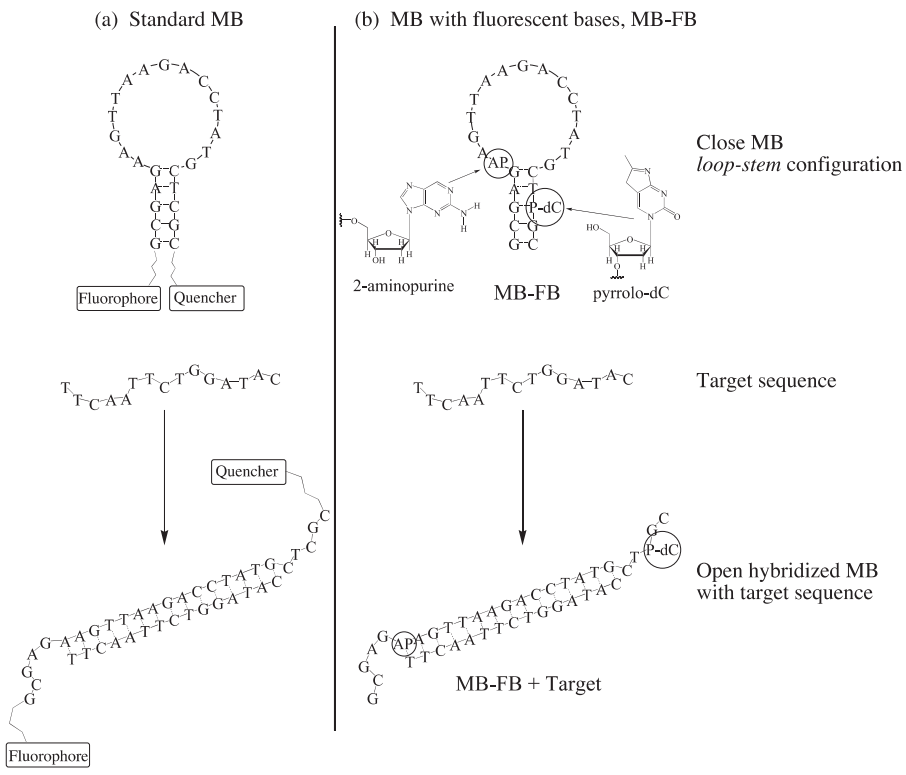

Scheme 1. Schematic structures of a standard MB (**a**) and a MB with FB (MB-FB) showing the position of the FB in circles (**b**).

normal oligonucleotide bases, displays an efficient fluorescence emission in solution ($\phi = 0.68$) (18). AP possesses a band in its absorption spectrum ($\lambda_{max} = 315$ nm) that is red shifted from the absorption spectra of the natural bases and a fluorescence emission with maximum at 370 nm. When AP is incorporated within an oligonucleotide chain its fluorescence decreases because of stacking interaction with neighbor bases within the strand (19). This decrease in fluorescence depends on the identity of the neighbors bases (20) of AP and the flexibility of the chain (21). The hybridization of a ss oligonucleotide containing AP to form the ds helical configuration decreases the fluorescence to an even greater extent owing to a more efficient stacking interaction among the bases (19). The lifetimes of AP range from a single monoexponential for the single nucleotide in solution ($\sim$9.3 ns) to four components exponential decay in ds DNA (e.g. 5 ps to >8 ns) (22). The shortest and longest components are related to totally stacked or unstacked configurations, respectively. AP has been used in the study of local interaction between DNA bases (20), electron transfer reactions along oligonucleotide strands (23,24) and ultraviolet (UV) damage in DNA (25).

A second fluorescent base that has been used for oligonucleotide studies is pyrrolo-dC (P-dC) (26). P-dC shares with AP a fluorescence sensitivity towards hybridization; however, the absorption peak ($\lambda_{abs} = 345$ nm) and fluorescence emission peak ($\lambda_{em} = 473$ nm) are red shifted in comparison with AP (27). P-dC has been successfully used in the study of the transcription bubble of T7 RNA polymerase (28,29). Besides, AP and P-dC, other FB are also available and their properties have been reviewed (16,17).

One of the advantages of FB is that they can be incorporated in the oligonucleotide backbone to produce DNA or RNA chains that are intrinsically fluorescent when ss but its fluorescence is strongly quenched when forming the double strand (17). The employment of these FB in the construction of MBs eliminates the use of a relatively large organic quencher externally attached to the oligonucleotide strand (compare Scheme 1a and b) since the backbone architecture itself provides the mechanism to tune their fluorescence properties. To the best of our knowledge, there is only one example in the literature in which a fluorescent base (AP) has been used to construct a MB like hybridization sensor (30). In this approach, AP was placed in either the loop or the stem. The fluorescence for this sensor increases up to 4.4 times when AP is in the stem and decreases up to 10 times when AP is in the loop (30). The major disadvantage of these sensors is that the maximum change because of hybridization with complementary strand corresponds to a decrease in fluorescence that implies a loss in the signal when it detects a complementary strand. This effect alone is undesirable for a MB sensor since the disappearance of the signal can be related to other factors such as dye decomposition or quenching, making the detection of complementary DNA ambiguous. Notwithstanding, Zhang *et al*. (10) had demonstrated that decreases and increases of different fluorescence signals can be used together to improve the detection sensitivity. Here, we report the synthesis and characterization of a MB using two FB: AP and P-dC. The combination of the signals of these two FB yields a sensitive fluorescence ratiometric detection of the complementary strand and at the same time imparts novel properties to the MB.

MATERIALS AND METHODS

MB-FB was prepared by solid phase phosphoramidite chemistry on an Expedite 8909 DNA synthesizer (Applied Biosystems). AP phosphoramidite and P-dC phosphoramidite were purchased from Glen Research (Sterling, VA). The resulting oligonucleotide was first purified using an oligonucleotide purification cartridge and then by high-performance liquid chromatography (31). To verify the identity and purity of the MB, matrix-assisted laser adsorption ionization/time of flight (MALDI-TOF) mass spectrometry (MS) was performed on the sample. The theoretical weight for MB-FB is 7729.3 Da which is very similar to the one obtained with MALDI-TOF MS of 7732.8 (*m*/*z*).

The concentration of MB-FB used for the fluorescence studies was 1.0 μM in 100 μM Tris–HCl buffer (pH 8.0) with 5 mM $MgCl_2$. Fluorescence excitation and emission measurements were performed at 25°C on a SPEX Fluorolog-3 spectrometer FL3-22 (J.Y. Horiba, Edison, NJ) using 5 nm slits and quartz cuvettes with an optical path length of 4 mm. The ratiometric fluorescence increase (RI) for MB-FB was determined using the following formula:

$$\mathrm{RI} = \frac{(I_{\mathrm{MBT,\,450nm}})/(I_{\mathrm{MB,\,450nm}})}{(I_{\mathrm{MBT,\,370nm}})/(I_{\mathrm{MB,\,370nm}})}, \qquad \mathbf{1}$$

where $I_{\mathrm{MBT,450}}$ and $I_{\mathrm{MB,450}}$ are the fluorescence intensity of MB-FB at 450 nm in the presence and in the absence of complementary strand respectively and $I_{\mathrm{MBT,370}}$ and $I_{\mathrm{MB,370}}$ are the fluorescence intensity of MB-FB at 370 nm in the presence and in the absence of complementary strand respectively. The excitation spectra were corrected for the non-homogeneous intensity of the excitation source by dividing the excitation signal by the signal of a reference detector (photodiode) placed after the excitation monochromator. Excitation spectra were corrected for DNA absorption using the following expression (25):

$$I_{\mathrm{C}} = I \times \mathrm{CF} \qquad \mathbf{2}$$

$$\mathrm{CF} = \frac{2.303 \times A(\lambda_{\mathrm{Exc.}})}{1 - 10^{-A(\lambda_{\mathrm{Exc.}})}}, \qquad \mathbf{3}$$

where I is the intensity at each wavelength of the spectrum, I_{C} is the corrected intensity at each wavelength of the spectrum, CF is the correction factor and $A(\lambda_{\mathrm{Exc.}})$ is the absorption intensity at each excitation wavelength. The UV-Vis spectra were collected with an Agilent 8456 spectrophotometer using quartz cuvettes of path length 4 mm. Time-resolved experiments were preformed on an OB900 single-photon counting Fluorometer (Edinburgh Analytical Instruments) with a pulsed nanosecond hydrogen lamp as excitation source.

RESULTS AND DISCUSSION

Design of MB with fluorescent bases (MB-FB)

MB-FB was synthesized based on a MB sequence reported by Tyagi *et al.* (9) with AP substituted for adenosine and P-dC substituted for cytosine in specific positions along the chain. Scheme 1b shows the MB-FB sequences and the position of the AP and P-dC FB in the oligonucleotide chain. The MB-FB synthesized is composed of a loop of 15 bases and a stem of 5 bases; the latter maintains the MB in the 'closed' configuration in the absence of the target sequence. Studies using AP and P-dC in different oligonucleotides show that these nucleotides form base pairs with T and G respectively in a similar way as their natural analogs without affecting significantly the structure of ds DNA (26,32). This condition is necessary since some base analogs destabilize the ds configuration of DNA, which can preclude the proper formation of the loop and stem structure of MB-FB.

Scheme 1b also shows the 'nucleotide' environment around the FB in both, the 'open' and 'closed' form of the MB-FB. In the 'closed' configuration AP is located in the ss loop while P-dC is located in the ds stem. On the other hand, when the MB is hybridized with its complementary strand, AP is in the ds form while P-dC is in the ss form. The positions of the bases in MB-FB were selected in order to provide two different microenvironments for the FB in the presence and absence of the target sequence. These different microenvironments are the product of the alternate hybridization of AP and P-dC when the MB is 'open' or 'closed' and result in a distinctive fluorescence signal for each of these states, depending on whether the MB is 'closed' or 'opened' by hybridization with its target.

Fluorescence response of MB-FB upon hybridization with its complementary sequence

The selectivity of a MB in detecting a defined oligonucleotide sequence is based on the characteristic change of its fluorescence response when it is exposed to the target sequence. An excess of target sequence (which causes a total hybridization of the MB) causes a maximum change in the MB fluorescence when compared with the fluorescence in the absence of the target sequence (9). In the case of MB-FB, excitation at 310 nm in the absence of the target sequence produces two distinctive fluorescence signals at 370 nm (strong) and 455 nm (weak) which correspond to the fluorescence of AP and P-dC respectively (solid line, Figure 1). In the ideal case, no fluorescence should be observed for P-dC because it is ds; however, transient dynamic conformations of the DNA bases within the ds conformation preclude the complete quenching of P-dC, leading to the occurrence of some fluorescence (33).

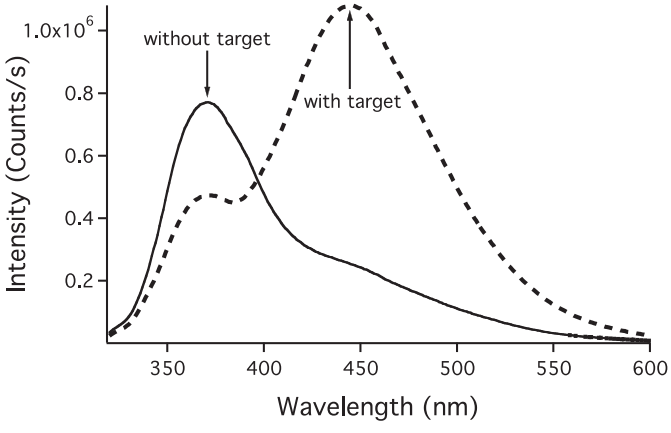

Figure 1. MB-FB fluorescence ($\lambda_{\mathrm{exc.}} = 310$ nm) without (solid line) and with (dashed line) an 3-fold excess of complementary strand.

Addition of 3-fold excess of the target sequence followed by 310 nm excitation produces a 1.8 times decrease in the emission of AP and a 4.5 times increase in the emission of P-dC (Figure 1). This behavior provides a recognition signature that contrasts with the standard MB in that it possesses a signal both in the 'closed' and in the 'open' configuration. This MB-FB presents characteristics similar to the two dye energy transfer (ET) MB reported by Zhang *et al.* (10) with the difference that for MB-FB the mechanism that produces the fluorescence change between the 'open' and 'close' forms is quenching by intra-strand interactions. In the case of AP, the MB changes from ss to ds when MB-FB hybridizes with its target sequence leading to decrease in fluorescence, while the opposite occurs for P-dC leading to fluorescence increase. The maximum ratiometric increase (see Equation 1, Materials and Methods) when an excess of target complementary strand is added to MB-FB (MB-FB&T) is ~8.5 when excited at 310 nm.

To obtain additional information about the quenching mechanism that controls the fluorescence emission in MB-FB, time-resolved fluorescence measurements were performed (Figure 2). Figure 2a shows the fluorescence decay kinetics for MB-FB in the absence and the presence of the target when the MB fluorescence is monitored at 380 nm (near AP emission maximum). Iterative reconvolution of the transients yielded biexponential fluorescence decays. The short lifetime component (~0.59 ns) should represent a variety of different short lifetime components due to stacked framework conformations that quench the fluorescence of AP. The component with a lifetime of ~6.5 ns (longest component) was assigned to mostly unstacked, ss AP, based on Larsen *et al.* (22). In the steady-state fluorescence experiments of MB-FB (without target) some fluorescence at 450 nm was observed, where P-dC shows its maximum fluorescence (Figure 1). Time resolved fluorescence experiments showed that the fluorescence decay at 450 nm (Figure 2b; without target) is almost identical to the fluorescence decay at 380 nm (Figure 2a). Therefore, we concluded that most of the fluorescence at 450 nm is attributed to the AP fluorescence. The contribution of P-dC fluorescence is negligible, confirming that in the absence of target, P-dC is strongly stacked with its neighbor bases resulting in efficient quenching of the fluorescence.

Addition of an excess of target to MB-FB causes a major change of the fluorescence decay kinetic at 450 nm, where P-dC fluoresces (Figure 2b). The long-lived component changes from 6.5 ns (55%) without target to 8.5 ns (87%) in the presence of target. Therefore, the fluorescence at 480 nm in the presence of target is mostly attributed to the fluorescence of P-dC. The addition of target scarcely affects the fluorescence decay profile or the fluorescence lifetimes of AP (monitored at 380 nm; Figure 2a).

Optimization of the ratiometric fluorescence

With the objective to find the optimum excitation wavelength yielding the maximum ratiometric increase in the fluorescence spectrum upon hybridization of MB-FB, we measured the excitation spectra of MB-FB in the presence and in the absence of its complementary strand (MB-FB&T). Figure 3a and b show the excitation spectra of MB-FB and MB-FB&T at 370 and 450 nm, respectively. The black curves in both spectra indicate the ratio of the spectrum after the addition of the complementary strand and before the addition of the complementary strand. These ratios indicate the local fluorescence change exciting at these wavelengths. However, to obtain the total ratiometric increase the change in fluorescence at 450 nm was divided by the change in fluorescence at 370 nm resulting in the curve shown in Figure 3c. This curve is equivalent to the plot of Equation 1 (Materials and Methods) as a function of the wavelength. The optimum excitation wavelengths obtained from Figure 3c are ~275 and 327 nm. Excitation at 325 nm yields a ratiometric change of 14 confirming the excitation spectra results (Figure 4). Excitation at 275 nm yields a slightly higher ratiometric change, however for practical applications this wavelength excitation is undesirable since it is within the spectral region were DNA bases present UV absorption.

Excitation spectra also provide photophysical information about AP and P-dC within MB-FB. A close inspection of the spectra in Figure 3a shows an unexpected band with maximum at ~270 nm. Bands at ~270 nm have been attributed to intra-strand FRET from neighbor bases to AP (21,34). This FRET mechanism was found to be more favorable for stacked bases, with adenosine nucleotides as the most efficient donors (25,35). Recent studies indicate that the spectroscopic parameters derived from oligonucleotides with AP can be used to probe local DNA conformations, which can provide a understanding of local interbase electronic interactions (22,35).

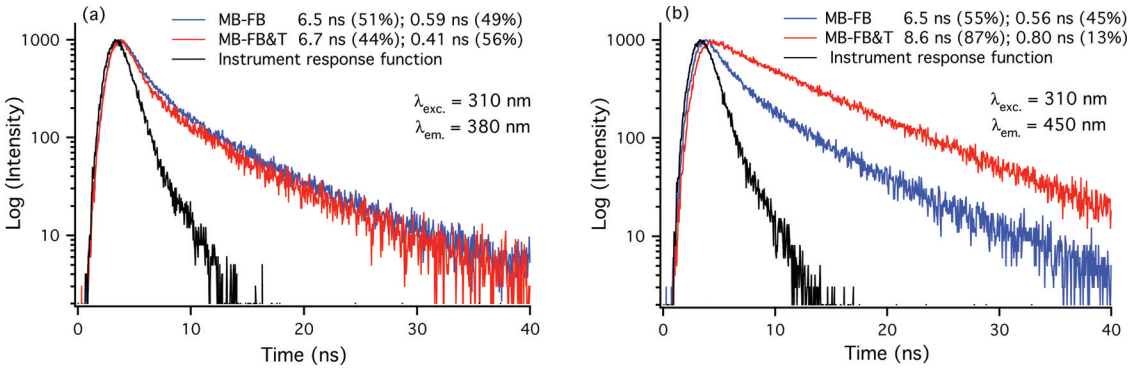

Figure 2. Fluorescence decay traces of MB-FB in the absence (blue curve) and in the presence of target (red curve) exciting at 310 nm and monitoring the emission at: (**a**) 370 nm and (**b**) 450 nm. The lifetimes are given in the legend with the respective abundances in parenthesis.

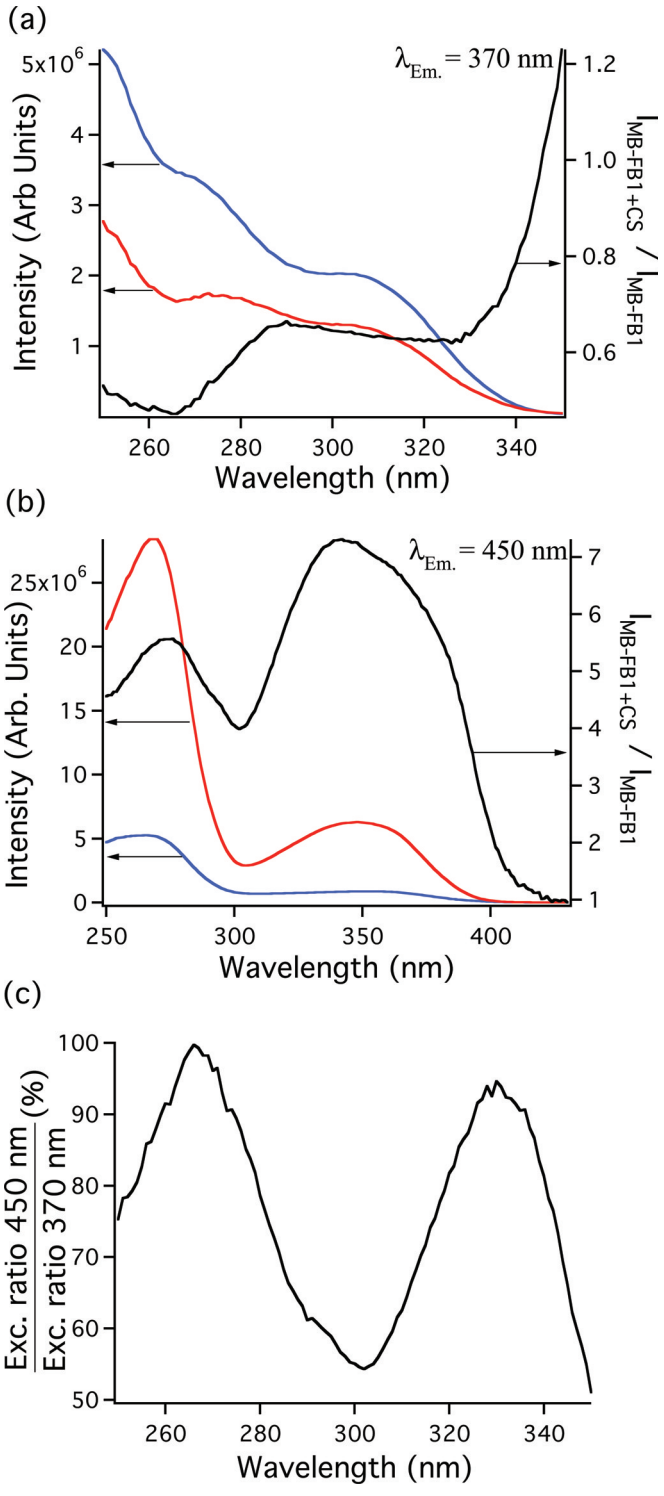

Figure 3. Excitation spectra of MB-FB at 370 nm (**a**) and 450 nm (**b**) in the absence (blue curve) and in the presence (red curve) of complementary strand. Ratio of the excitation spectrum in the presence and absence of complementary strand (black curve). (**c**) Total ratiometric increase (as defined by Equation 1).

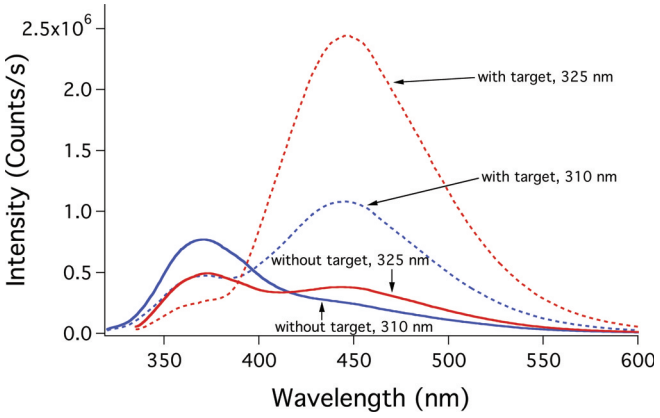

Figure 4. Emission spectra of MB-FB with excitation at 310 nm (blue) and 325 nm (red) without (solid line) and with (dashed line) a 3 fold excess of complementary strand.

At this point, it is important to note that two different interbase interactions producing different spectroscopic features can occur in oligonucleotides with stacked AP. By interbase interactions we refer to the electronic interactions between the bases (fluorescent and non fluorescent) that are reflected in the fluorescence spectra of AP and P-dC.

In order to extract the maximum information from Figures 1 and 3 it is necessary to distinguish between the two different inter-base interactions and how they affect the photophysical properties of MB-FB. The first interaction is the one responsible for the decrease in the AP fluorescence when AP switches its conformation from ss to ds. This interaction was modeled by Jean and Hall, assuming stacking of the bases in a B-DNA configuration and concluded that AP quenching by A and G bases is due to a ground state mixing of the orbitals of these bases with AP (19). On the other hand, the same researchers found that the quenching of AP by T or C is due to the formation of a non-fluorescent complex between AP and these bases (19). This behavior is reflected in Figure 1 by the decrease in intensity of AP after the addition of complementary DNA. The decrease in fluorescence of AP observed going from ss to ds has been attributed to a more efficient stacking of the bases when AP is in the ds form (18,36). P-dC is also influenced by this interbase interaction. Excitation of P-dC at 370 nm yields only the emission spectrum of P-dC (without any contribution from AP) showing a 7 times increases in its fluorescence when complementary strand is added. As was stated before, this corresponds to a change from ds to ss for P-dC, which confirms once again the sensitivity of this probe to the oligonucleotide microenvironment. This appears to be the largest change in the fluorescence of P-dC ever reported thus far (28,29).

The second type of interaction produces an intra-strand FRET from neighbors bases to AP, which is characterized by a band in the excitation spectrum at ~270 nm (34). This interaction has been also associated to the stacking of the DNA bases; however in this case the FRET is not dependent on whether the oligonucleotide is ss or ds (25). On the other hand, it has been reported that an increase in temperature effectively quenches the 270 nm band, which is due to unstacking of AP and its neighbor nucleotides (21). Figure 3a shows a band at ~270 nm for MB-FB in the presence and in the absence of the target sequence. The appearance of this band is consistent with the second kind of inter-base interaction and indicates that AP is strongly stacked with adenine either in the presence or in the absence of

complementary strand. The data in Figure 3a also show a decrease in the intensity of the excitation spectrum after addition of complementary strand that corresponds to the first kind interbase interaction, i.e. quenching of AP excited state. Similarly, the increase in intensity of P-dC upon addition of complementary strand is observed as shown in Figure 3b, which is because of the first kind of interbase interaction as in the case of AP.

Local configuration and interaction of nucleotide bases within MB-FB by thermal denaturation profile analysis

The use of FB to construct MB provides an opportunity to study local configuration and interaction of the nucleotide bases at defined sites within the MB. In contrast to the changes in the UV-Vis measurements, which represent an average of all the nucleic acids in the sample, the use of FB allows the measurements to be focused in a specific nucleotide within the MB.

Figure 5 shows the thermal denaturation profiles for P-dC in MB-FB. The curve for MB-FB in the absence of template presents the classic S shape curve for DNA, with a marked increase in the fluorescence intensity when the temperature is increased indicating a cooperative mechanism in the denaturation of the MB (Figure 5a). The melting point extracted from the curve is ~53°C. This observation confirms that MB-FB is in the 'closed' configuration at ambient temperature. The marked increase in the fluorescence intensity also indicates that P-dC is acting as a probe for the stem of MB-FB, which is expected since P-dC is positioned exactly at the center of the stem when MB-FB is in a 'closed' conformation.

The addition of 3-fold excess of target template to the MB causes the expected rise in fluorescence. Increasing the temperature causes an initial constant decrease in the fluorescence that is due to the decrease in the P-dC quantum yield with the temperature. Further increases in the temperature produce a marked decrease in the fluorescence intensity corresponding to the transition from ds to ss random coil (Figure 5b). Since P-dC was already ss the latter fluorescence drop is unexpected. ss DNA shows non-cooperative denaturation profiles characterized by slow rising (or decreasing as in this case) S shape curves (37). The observation of a marked P-dC fluorescence decrease indicates that the ds part in MB-FB&T, in addition to prevent the MB from closing, also plays other roles that help to preserve the strong luminescence of P-dC in this configuration. One of the possibilities is that the rigid structure of the ds helix prevents P-dC from interacting with the main body of the MB. When MB-FB&T is heated to a temperature high enough to breakup the base pair interactions, the oligonucleotide chain becomes a flexible ss random coil. The random coil flexibility allows P-dC to interact with internal oligonucleotides increasing the probability of collisions and subsequently decreasing the fluorescence intensity by collisional quenching.

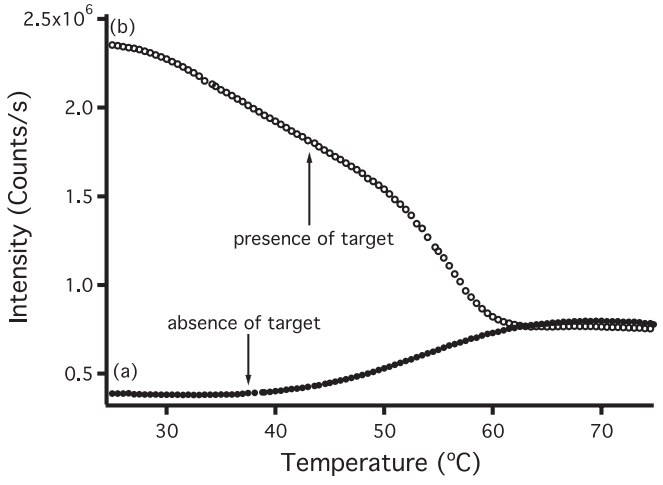

Figure 5. Fluorescence as a function of temperature for MB-FB in the absence (**a**) and in the presence (**b**) of complementary strand ($\lambda_{exc.} = 370$ nm, $\lambda_{em.} = 450$ nm).

CONCLUSIONS

We have designed a novel MB possessing intrinsically FB, which displays an enhanced sensitivity for the detection of complementary DNA and also displays interesting photophysical properties. Such a MB possesses the advantage over standard MBs that is very easy to synthesize and purify. In contrast, an advantage of standard MBs is that there are more organic dyes available for the MB synthesis than intrinsically FB. However, in the last few years, additional fluorescent nucleotides have been reported with a variety of photophysical properties which can be explored to construct MBs with novel properties (16,17,38–40). In addition, we demonstrated that the excitation wavelength of MB-FB can be optimized to display a fluorescent ratiometric increase larger than when excited at its absorption maximum. The smaller size of these sensors and the fact that they are structurally similar to normal DNA compared with standard MB can improve the diffusion and recognition of these sensors in different media. In addition, this kind of MB does not possess dyes or quenchers attached to the 5′ or 3′ end, which can interfere with other molecules in the media or being detached from the chain producing false signals. This sensor has the potential for wide applications such as real time PCR assays, DNA–protein interaction experiments and nucleic acid hybridization studies. This approach can also be used within the architecture of standard MBs to study local conformation of MBs and increase the fluorescence contrast ratio between the non-hybridized and hybridized states. Finally, this MB presents the first example of a MB with two fluorophores in which the first dye fluoresce while the second is quenched in the absence of target and vice versa in the presence of target (the second dye fluoresce while the first is quenched). However, in spite of the mentioned advantages of MB-FB, they are not intended to substitute the standard MB but to provide a novel perspective in the design of these kinds of sensors.

ACKNOWLEDGEMENTS

This work was supported by the Center of Excellence in Genomic Science Grant P50 HG002806 from the National Institutes of Health and NSF CHE-04-15516. Funding to

pay the Open Access publication charges for this article was provided by the Center of Excellence in Genomic Science Grant P50 HG002806 from the National Institutes of Health.

Conflict of interest statement. None declared.

REFERENCES

1. McGown,E., Su,M. and Dennis,R. (2000) Measurements of molecular beacons in the SpectraMax GEMINI spectrofluorometer. *J. Chem. Technol. Biotechnol*., **75**, 942–944.
2. Mhlanga,M.M., Vargas,D.Y., Fung,C.W., Kramer,F.R. and Tyagi,S. (2005) tRNA-linked molecular beacons for imaging mRNAs in the cytoplasm of living cells. *Nucleic Acids Res*., **33**, 1902–1912.
3. Peng,X.-H., Cao,Z.-H., Xia,J.-T., Carlson,G.W., Lewis,M.M., Wood,W.C. and Yang,L. (2005) Real-time detection of gene expression in cancer cells using molecular beacon imaging: new strategies for cancer research. *Cancer Res*., **65**, 1909–1917.
4. Bergeron,M.G. and Ke,D. (2001) New DNA-based PCR approaches for rapid real-time detection and prevention of group B streptococcal infections in newborns and pregnant women. *Exp. Rev. Mol. Med*., 1–14.
5. Tsourkas,A. and Bao,G. (2003) Shedding light on health and disease using molecular beacons. *Brief. Funct. Genomic Proteomic*, **1**, 372–384.
6. Tan,W., Wang,K. and Drake,T.J. (2004) Molecular beacons. *Curr. Opin. Chem. Biol*., **8**, 547–553.
7. Tan,W., Fang,X., Li,J. and Liu,X. (2000) Molecular beacons: a novel DNA probe for nucleic acid and protein studies. *Chem. Eur. J*., **6**, 1107–1111.
8. Bonnet,G., Tyagi,S., Libchaber,A. and Kramer,F.R. (1999) Thermodynamic basis of the enhanced specificity of structured DNA probes. *Proc. Natl. Acad. Sci. USA*., **96**, 6171–6176.
9. Tyagi,S. and Kramer,F.R. (1996) Molecular beacons: probes that fluoresce upon hybridization. *Nat. Biotechnol*., **14**, 303–308.
10. Zhang,P., Beck,T. and Tan,W. (2001) Design of a molecular beacon DNA probe with two fluorophores. *Angew. Chem. Int. Ed*., **40**, 402–405.
11. Fujimoto,K., Shimizu,H. and Inouye,M. (2004) Unambiguous detection of target DNAs by excimer-monomer switching molecular beacons. *J. Org. Chem*., **69**, 3271–3275.
12. Nutiu,R. and Li,Y. (2002) Tripartite molecular beacons. *Nucleic Acids Res*., **30**, e94.
13. Brown,L.J., Cummins,J., Hamilton,A. and Brown,T. (2000) Molecular beacons attached to glass beads fluoresce upon hybridization to target DNA. *J. Chem. Soc. Chem. Comm*., 621–622.
14. Silverman,A.P. and Kool,E.T. (2005) Quenched probes for highly specific detection of cellular RNAs. *Trends Biotechnol*., **23**, 225–230.
15. Masuko,M., Ohtani,H., Ebata,K. and Shimadzu,A. (1998) Optimization of excimer-forming two-probe nucleic acid hybridization method with pyrene as a fluorophore. *Nucleic Acids Res*., **26**, 5409–5416.
16. Hawkins,M.E. (2001) Fluorescent pteridine nucleoside analogs. *Cell Biochem. Biophys*., **34**, 257–281.
17. Rist,M.J. and Marino,J.P. (2002) Fluorescent nucleotide base analogs as probes of nucleic acid structure, dynamics and interactions. *Curr. Org. Chem*., **6**, 775–793.
18. Ward,D.C., Reich,E. and Stryer,L. (1969) Fluorescence studies of nucleotides and polynucleotides. *J. Biol. Chem*., **244**, 1228–1237.
19. Jean,J.M. and Hall,K.B. (2001) 2-Aminopurine fluorescence quenching and lifetimes: role of base stacking. *Proc. Natl. Acad. Sci. USA*., **98**, 37–41.
20. Rachofsky,E.L., Osman,R. and Ross,J.B.A. (2001) Probing structure and dynamics of DNA with 2-aminopurine: effects of local environment on fluorescence. *Biochemistry*, **40**, 946–956.
21. Kawai,M., Lee,M.J., Evans,K.O. and Nordlund,T.M. (2001) Temperature and base sequence dependence of 2-aminopurine fluorescence bands in single- and double-stranded oligodeoxynucleotides. *J. Fluoresc*., **11**, 23–32.
22. Larsen,O.F.A., van Stokkum,I.H.M., Gobets,B., van Grondelle,R. and van Amerongen,H. (2001) Probing the structure and dynamics of a DNA hairpin by ultrafast quenching and fluorescence depolarization. *Biophys. J*., **81**, 1115–1126.
23. Wan,C., Fiebig,T., Schiemann,O., Barton,J.K. and Zewail,A.H. (2000) Femtosecond direct observation of charge transfer between bases in DNA. *Proc. Natl. Acad. Sci. USA*., **97**, 14052–14055.
24. Kelley,S.O. and Barton,J.K. (1999) Electron transfer between bases in double helical DNA. *Science*, **283**, 375–381.
25. Xu,D.-G. and Nordlund,T.M. (2000) Sequence dependence of energy transfer in DNA oligonucleotides. *Biophys. J*., **78**, 1042–1058.
26. Berry,D.A., Jung,K.-Y., Wise,D.S., Sercel,A.D., Pearson,W.H., Mackie,H., Randolph,J.B. and Somers,R.L. (2004) Pyrrolo-dC and pyrrolo-C: fluorescent analogs of cytidine and 2′-deoxycytidine for the study of oligonucleotides. *Tetrahedron Lett*., **45**, 2457–2461.
27. Thompson,K.C. and Miyake,N. (2005) Properties of a new fluorescent cytosine analogue, pyrrolocytosine. *J. Phys. Chem. B*, **109**, 6012–6019.
28. Liu,C. and Martin,C.T. (2002) Promoter clearance by T7 RNA polymerase. *J. Biol. Chem*., **277**, 2725–2731.
29. Liu,C. and Martin,C.T. (2001) Fluorescence characterization of the transcription bubble in elongration complexes of T7 RNA polymerase. *J. Mol. Biol*., **308**, 465–475.
30. Kourentzi,K.D., Fox,G.E. and Willson,R.C. (2003) Hybridization-resposive florescent DNA probes containing the adenine analog 2-aminopurine. *Anal. Biochem*., **322**, 124–126.
31. Bai,X., Li,Z., Jockusch,S., Turro,N.J. and Ju,J. (2003) Photocleavage of a 2-nitrobenzyl linker bridging a fluorophore to the 5′ end of DNA. *Proc. Natl. Acad. Sci. USA*., **100**, 409–413.
32. Rai,P., Cole,T.D., Thompson,E., Millar,D.P. and Linn,S. (2003) Steady-state and time-resolved fluorescence studies indicate an unusual conformation of 2-aminopurine within ATAT and TATA duplex DNA sequences. *Nucleic Acids Res*., **31**, 2323–2332.
33. Guest,C.R., Hochstrasser,R.A., Sowers,L.C. and Millar,D.P. (1991) Dynamics of mismatched base pairs in DNA. *Biochemistry*, **30**, 3271–3279.
34. Nordlund,T.M., Xu,D. and Evans,K.O. (1993) Excitation energy transfer in DNA: duplex melting and transfer from normal bases to 2-aminopurine. *Biochemistry*, **32**, 12090–12095.
35. Davis,S.P., Matsumura,M., Williams,A. and Nordlund,T.M. (2003) Position dependence of 2-aminopurine spectra in adenosine pentadeoxynucleotides. *J. Fluoresc*., **13**, 249–257.
36. Law,S.M., Eritja,R., Goodman,M.F. and Breslauer,K.J. (1996) Spectroscopic and calorimetric characterizations of DNA duplexes containing 2-aminopurine. *Biochemistry*, **35**, 12329–12337.
37. Voet,D. and Voet,J.G. (1995) *Biochemistry. 2nd edn*. Wiley & Sons, New York.
38. Jameson,D.M. and Eccleston,J.F. (1997) Fluorescent nucleotide analogs: synthesis and applications. *Methods Enzymol*., **278**, 363–390.
39. Hawkins,M.E. (2003) Fluorescent nucleoside analogues as DNA probes. In Lakowicz,J.R. (ed.), *DNA Technology*. Kluwer Academic/Plenum Publishers, New York, Vol. 7, pp. 151–175.
40. Cremo,R.C. (2003) Fluorescent nucleotides: synthesis and characterization. *Methods Enzymol*., **360**, 128–177.